

Influence of dissolved gas concentration on the lifetime of surface bubbles in volatile liquids

Xin Li^a, Yanshen Li^{a,b,*}

^a*School of Engineering Science, University of Chinese Academy of Sciences, Beijing, 101408, PR China*

^b*State Key Laboratory of Nonlinear Mechanics, Institute of Mechanics, Chinese Academy of Sciences, Beijing, 100190, PR China*

Abstract

Bubbles at the air-liquid interface are important for many natural and industrial processes. Factors influencing the lifetime of such surface bubbles have been investigated extensively, yet the impact of dissolved gas concentration remains unexplored. Here we investigate how the lifetime of surface bubbles in volatile liquids depends on the dissolved gas concentration. The bubble lifetime is found to decrease with the dissolved gas concentration. Larger microbubbles at increased gas concentration are found to trigger bubble bursting at earlier times. Combined with the thinning rate of the bubble cap thickness, a scaling law of the bubble lifetime is developed. Our findings may provide new insight on bubble and foam stability.

Keywords: surface bubbles, lifetime, dissolved gas concentration, microbubbles

1. Introduction

Bubbles are omnipresent in nature and industrial applications, such as in floatation (Peleka et al., 2018), renewable energy production (Ardo et al., 2018; Chatenet et al., 2022), inkjet printing (Lohse, 2022), thermal management (Mohanty and Das, 2017; Yang et al., 2023), ultrasound diagnostics (Dollet et al., 2019), etc. For comprehensive reviews on bubbles, we refer to Lohse (2018) and Garbin et al. (2025).

Among them, bubbles at the air/liquid interface, also called surface bubbles, are important for climate change and food industry. For example, when bubbles on the sea surface burst, they release aerosols into the atmosphere (Lhuissier and Villermaux, 2012; Lohse and Villermaux, 2020), which influences the air-sea mass exchange (Deike, 2022). In carbonated beverages, surface bubbles may form a layer of foam, whose quality is crucial for the flavor and visual appeal of the beverage (Viejo et al., 2019). In bath and cleaning products, surface bubbles amplify detergent-dirt contact, boosting cleaning efficiency and user comfort (Jin et al., 2022). The stability and lifetime of surface bubbles are found vital to these applications. Thus, extensive studies have investigated factors that influence the lifetime of surface bubbles. Surfactants were found to

increase the lifespan of surface bubbles, presumably because they make the liquid/air solid-like, which hinders film drainage due to gravity (Sonin et al., 1993; Adami and Caps, 2015). Temperature gradients or concentration gradients, caused by evaporation (Menesses et al., 2019; Lorenceau and Rouyer, 2020) or imposed directly (Nath et al., 2022), could also increase the lifetime by introducing Marangoni flows on the bubble cap, which compensates for the film drainage. Viscosity also increases the lifetime by directly slows the film drainage (Debrégeas et al., 1998; Oratis et al., 2020). Salinity was found to influence the bubble lifetime in a non-monotonic way (Magdalena and Pablo, 2017). However, among all the factors that influence the surface bubble lifetime, the impact of dissolved gas concentration has not been explored, even though it is strongly relevant in the food industry.

We investigate the influence of dissolved gas concentration on the lifetime of surface bubbles in volatile liquids. The dissolved gas concentrations are varied by depressurizing or pressurizing the liquid. Dissolved oxygen concentrations are measured to represent the dissolved gas concentrations. Surface bubbles are generated by injecting 90 μL air into the bulk liquid and let it rise. Lifetime of surface bubbles are found to decrease while increasing the dissolved gas concentration. After analyzing the recorded bursting events, we find that bubble bursting is triggered by large enough microbub-

*Email address for correspondence: liyanshen@ucas.ac.cn

bles in the thin film of the bubble. We also find that the average microbubble diameter increases almost linearly with the dissolved gas concentration. Combined with the thinning rate of the film thickness, a scaling law is developed to explain the dependence of surface bubble lifetime on the dissolved gas concentration.

2. Experimental procedures and methods

At room temperature, a petri dish (STEENA, China) of diameter 3.5 cm and depth 10 mm were filled with liquids of different dissolved gas concentration. Isopropanol (Mreda, purity 99.5 %) was used as the liquid. The petri dish was rinsed with ethanol and deionized water (Hhitech, Master Touch-RUV, China) then dried with compressed air beforehand. As depicted in Fig. 1, a needle of inner diameter 0.51 mm was immersed in the liquid, which was connected to a syringe mounted on a syringe pump (Leadfluid, TFD02, China). An air bubble of volume 90 μL was injected at a flow rate 42.75 mL/min so as to form a hemispherical bubble at the surface. A short plastic tube shorter than the liquid depth was placed at the center of the petri dish to prevent the surface bubble from moving around. A collimated LED (Thorlabs, LEDD1B, USA) and a camera (Nikon D850, at 60 fps and 1920 \times 1080 resolution) connected with a long working distance zoom lens system (Thorlabs, MVL12X12Z plus 2X lens attachment, USA) were used to record the life time t_l of the bubble.

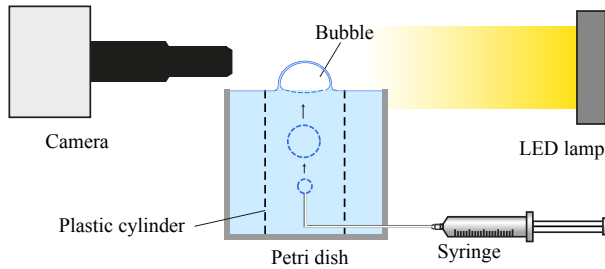


Fig. 1. This apparatus is designed to investigate the dynamic behavior of bubbles at liquid surfaces. Bubbles are generated by injecting air at a constant flow rate through a 0.5 mm inner diameter needle below the liquid surface, with a plastic cylinder employed to constrain horizontal bubble movement.

To control the dissolved gas concentration of the liquids, different methods were used for undersaturated and oversaturated liquids. For undersaturation, around 100 mL liquid was put in a vacuum-desicator at around 1000 Pa for 5 to 30 min to control its gas concentration. For oversaturation, around 100 mL liquid was put in a

pressurized container at 2 to 6 bar for 2 to 24 h. Then the undersaturated or oversaturated liquid was poured into another container to measure its dissolved oxygen concentration c_o by an optical dissolved oxygen meter (Mettler-Toledo, S900-K, USA). It takes about 30 s to measure the dissolved oxygen concentration c_o in the liquid. Right after the c_o has been measured, the liquid was filled into the petri dish to start the experiment. To minimize the change of gas concentration in the liquid due to the gas exchange with air during the experiments, the undersaturated (oversaturated) liquid was used for no longer than 5 min (2 min), because it was found that within these time intervals, the gas concentration in the liquid does not change much (see Supplementary Materials for details).

To capture the detailed rupture processes of the bubbles, a high speed camera (Photron, Nova S12, Japan) at frame rates ranging from 3000 to 25 000 fps was used instead. Liquid film thickness h of the bubble at the instance of rupture was calculated using the Taylor-Culick method (Taylor, 1956; Botta et al., 2020):

$$h = \frac{2\sigma}{\rho v^2}, \quad (1)$$

where σ is the surface tension and ρ is the density of the liquid, v is the retraction speed of the edge of the hole in the film, which is measured by the recorded high speed video. The initial film thickness h_i of the bubble was also measured using this method by puncturing the bubble with a needle immediately after it is generated. The density and surface tension of isopropanol at 25 $^{\circ}\text{C}$ and 1 atm are 0.781 g/cm³ and 20.4 mN/m (Haynes, 2016), respectively.

3. Results and discussions

The influence of liquid gas concentration, represented by the oxygen concentration c_o , on the bubble lifetime t_l is shown in Fig. 2. The data are collected from 363 experiments. It is clearly shown that the surface bubble lifetime t_l decreases as the dissolved gas concentration in the liquid increases. Especially, the bubble lifetime in the undersaturated liquid (red squares) decreases sharply as the gas concentration increases. As the dissolved gas becomes saturated (green circles), the bubble lifetime starts to decrease slowly. This trend continues until the liquid is oversaturated (blue triangles).

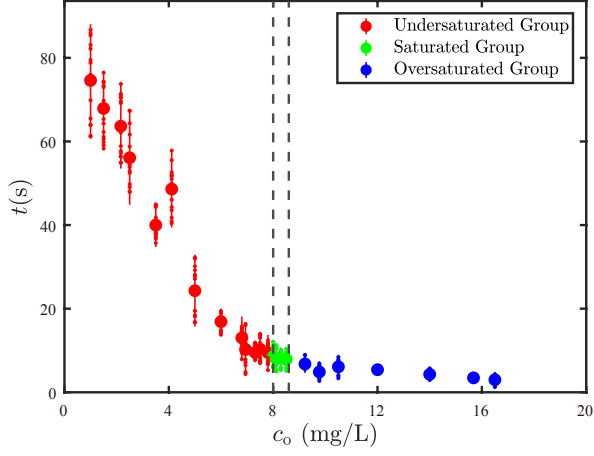


Fig. 2. (a) Average lifetime $\langle t \rangle$ of anhydrous ethanol bubbles as a function of c_o , (b) Average lifetime $\langle t \rangle$ of isopropanol bubbles as a function of c_o . The horizontal axis denotes c_o (unit: mg/L), and the vertical axis represents average lifetime (unit: s). Red, green, and blue indicate undersaturated, saturated, and oversaturated states, respectively, with each data point representing the mean of 10–15 bubbles.

Surface bubbles are made of air enclosed by a thin layer of liquid, which is vital to the bubble lifetime. The rupture of surface bubbles can be divided into two stages (Poulain et al., 2018): (i) Deterministic thinning of the liquid film due to gravity. (ii) Rupture of the film due to internal or external disturbances, which ruptures the film by nucleating a hole large enough in the liquid film. Of all the factors that influence the thinning of the liquid film (Menesses et al., 2019; Lorenceau and Rouyer, 2020; Nath et al., 2022; Debrégeas et al., 1998; Oratis et al., 2020), dissolved gas concentration does not seem to influence any of them. Thus, we speculate that the increased gas concentration in the liquid does not influence the film thinning process, but affects the surface bubble lifetime by bringing strong enough disturbances earlier to the film, consequently leading to its earlier rupture. This speculation is supported by measuring the initial film thickness h_i of the isopropanol bubbles and the film thickness at rupture h_r . The film thicknesses are measured by Taylor-Culick method, see Section 2. The initial film thickness h_i is measured by puncturing the bubble with a needle right after it is generated. Fig. 3(a) shows the initial film thickness h_i of the surface bubbles at different dissolved gas concentrations. It is clear that the initial film thickness of the bubbles do not vary with the dissolved gas concentration, and the average value is found to be $h_i \approx 0.93 \mu\text{m}$. Fig. 3(b) shows the film thickness h_r of the bubbles at rupture. It can be seen that as the dissolved gas concentration increases,

the film thickness at rupture h_r also increases. This suggests that by increasing the dissolved gas concentration, the bubble lifetime's decrease is due to early rupture of the film. Notice that the largest film thickness at rupture is $h_r = 0.8 \mu\text{m}$, smaller than the initial film thickness $0.93 \mu\text{m}$.

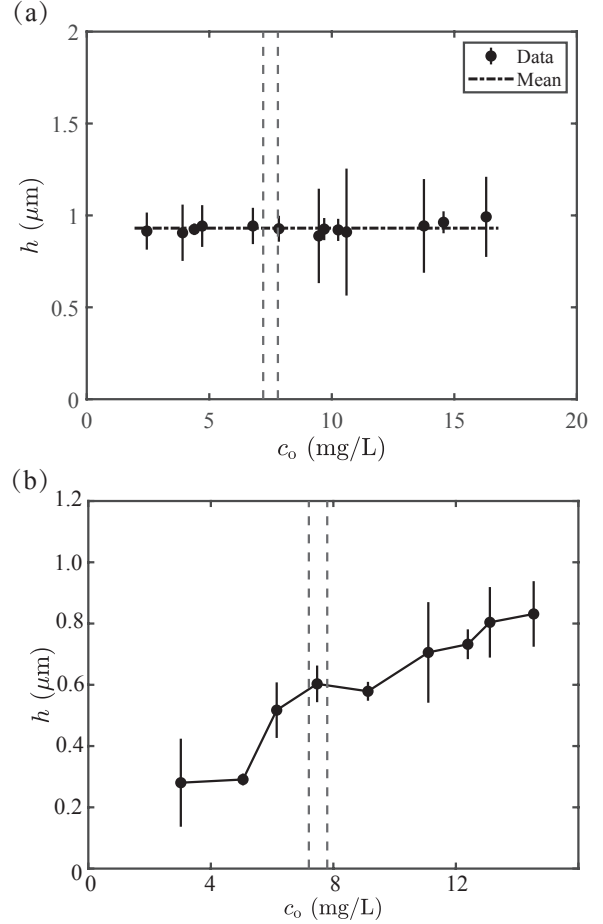


Fig. 3. Initial film thickness h_s of isopropanol bubbles under different c_o conditions, each point averaging 15 bubbles, with the red line indicating the overall mean ($h_s \approx 0.93 \mu\text{m}$). The dashed line denotes the saturation boundary at standard temperature and pressure.

We then observe the bubble closely to see what triggers the rupture of the film. It was found that a small particle rising in the film is responsible for the initiation of the hole and the subsequent rupture, see Fig. 4 for a typical rupture event recorded by the high speed camera (see also Movie S1). As can be seen, a small particle (the black dot) first rises in the liquid film from the bottom of the bubble (from $t = 0$ ms to 0.24 ms). Immediately after (0.04 ms later), a hole appears at the

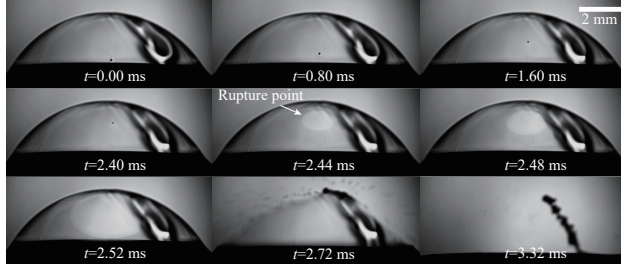


Fig. 4. Snapshots of a rupture event of an isopropanol bubble. The liquid is oversaturated and its dissolved oxygen concentration is $c_o = 9.33$ mg/L. A small particle (the black dot) rises from the bottom to the liquid film (from $t = 0$ ms to 0.24 ms), immediately after (0.04 ms later), a hole appears and expands at the position of the particle, which later leads to the rupture of the bubble. Scale bar is 2 mm.

position of the particle. This hole expands due to surface tension, which finally leads to the rupture of the film. These snapshots show that this single rupture event was triggered by internal disturbances induced by the particle. In order to find out the probability of bubble bursts due to the same reason, i.e., caused by a particle, more bursting events at different dissolved gas concentrations are recorded. Those with a clear evidence that the rupture was triggered by a particle (similar to that show in Fig. 4) were counted, and the probability is shown in Fig. 5. It is found that 64 out of 69 bursting events are confirmed to be triggered by a particle, giving an overall probability of 92.8 %. The real probability of particle-triggered-bursting should be larger than this value, because in some cases the particle is not visible to the camera and thus not counted. For example, when the particle trajectory happens to be overlapping with the bubble's outline, it cannot be recorded by the camera.

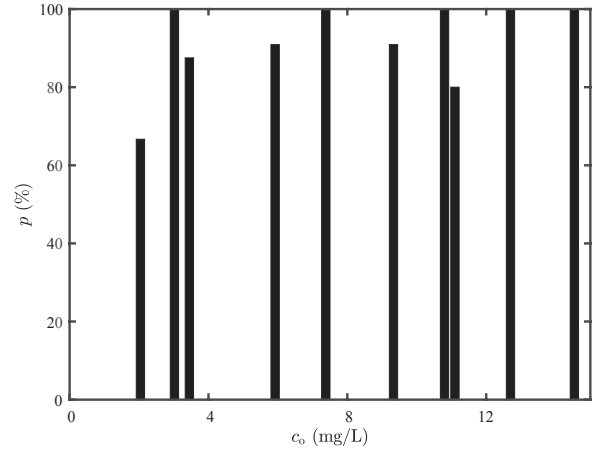


Fig. 5. Statistical histogram of the proportion of isopropanol bubble ruptures attributed to microbubbles under varying c_o conditions, based solely on bubbles with clearly observable frontal perforations.

Nevertheless, the probability of particle-triggered-bursting being larger than 92.8 % further confirms our speculation that a larger dissolved gas concentration decreases the bubble lifetime by bringing an early rupture of the film. The next question arises naturally, that is, what is the essence of the particles? They could be solid particles due to impurities in the liquid, or they could be microbubbles. But one could be easily tell that they are actually microbubbles mainly due to two reasons: First, all the particles observed are spherical, while solid impurities are often irregular in shape (Poulain et al., 2018). Second, upon film rupture, the particle suddenly “disappears” and no trace of impurities are observed in the film close to the hole. This suggests the gaseous nature of the particle. It might seem counterintuitive at first sight for undersaturated liquid to have microbubbles in the bulk, but Fang et al. (2018) has shown that stable bulk nanobubbles could exist in undersaturated liquids. We also observed microbubbles in the bulk of undersaturated (and also oversaturated) liquids.

The diameters of the microbubbles d are measured by monitoring the central region of the bubble, see Fig. 6. The red box in the inset shows the monitored region. It can be seen that the average diameter of the microbubbles \bar{d} increases with the dissolved gas concentration (represented by the oxygen concentration c_o) almost linearly. This can be explained as follows. These microbubbles nucleate in the bulk liquid and grow until they reach the surface. Some of them could enter the film of the surface bubble and continue to rise. But given the very short duration when the microbubbles are

in the bubble cap (2.4 ms for example, see Fig. 4), their size change in the bubble cap can be neglected. Thus, the microbubbles only grow in size when they are in the bulk. We then estimate the average diameter of the microbubble. The nucleation of the microbubbles can be seen as a random process, and the probability of a nucleus to appear in certain position can be considered as uniform throughout the bulk liquid. Then, the average residence time of the microbubbles in liquids with different dissolved gas concentration is assumed to be the same. Further assuming that the growth of the microbubble is dictated by diffusion (given their small size and small rising velocity), we have $\bar{d} \sim c_o$ according to Epstein and Plesset (1950).

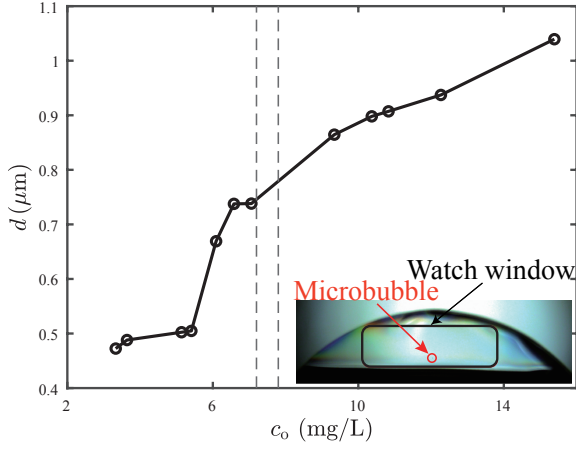


Fig. 6. Diameter $\langle d \rangle$ (left y-axis, black line) and frequency f (right y-axis, green line) of microbubbles in the late stage of isopropanol bubble lifetime at different dissolved gas concentration represented by c_o . Each green point represents the mean diameter of 1–5 suspected microbubbles.

Now we further analyze the dependence of bubble lifetime on dissolved gas concentration. The microbubbles must be large enough to trigger the rupture of the film. It is then reasonable to assume that the film will definitely rupture if the (average) microbubble diameter is larger than the film thickness by a certain factor. Or in other words, $\bar{d}/h_r \approx k$ where $k > 1$ is the factor. Actually, this can be confirmed by comparing the microbubble diameter shown in Fig. 6 with the film thickness at rupture shown in Fig. 3(b). For example, the average bubble diameter at $c_o \approx 12$ mg/L is $d \approx 0.9 \mu\text{m}$, larger than the film thickness at rupture $h_r \approx 0.7 \mu\text{m}$. Coming back to the analysis, $\bar{d}/h_r \approx k$ also means that $\bar{d} \sim h_r$. Because $\bar{d} \sim c_o$, we have $h_r \sim c_o$ (see Fig. 3(b)). For volatile liquids, it has been found that the film thickness of a surface bubble follows $h \sim t^{-2/3}$ (Lhuissier and

Villermaux, 2012; Poulain et al., 2018). So at the instant when the film ruptures, it follows $h_r \sim t_l^{-2/3}$. Substituting the dependence of film thickness at rupture h_r on the dissolved gas concentration, we obtain $t_l \sim c_o^{-3/2}$. The bubble lifetime data shown in Fig. 2 is replotted as the red dots in Fig. 7 in log-log scale. Another set of experiments were performed several months later, as shown by the black squares. It is found that this scaling law $t_l \sim c_o^{-3/2}$ fits the two sets of experimental results well.

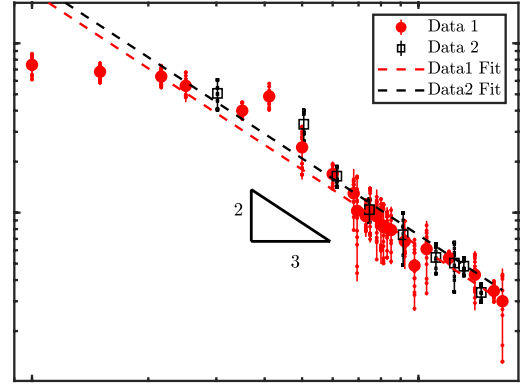


Fig. 7. Lifetime of the surface bubble t_l at different dissolved oxygen concentrations c_o in log-log scale. The dashed line has a slope of $-3/2$.

4. Conclusions

In summary, we have investigated how the surface bubble lifetime t_l in volatile liquids depends on the dissolved gas concentration, which is represented by the oxygen concentration c_o . The initial film thickness of the bubble cap is found to be $h_i \approx 0.93 \mu\text{m}$, independent of the dissolved gas concentration. Yet the film thickness at rupture increases with the dissolved gas concentration. High speed recordings reveal that microbubbles are responsible for the film rupture. Further, it is found that larger microbubbles at increased gas concentration trigger bubble bursting at earlier times, thus leading to a decrease in the bubble lifetime. Combined with the film thinning rate of surface bubbles in volatile liquids, we found that the dependence of bubble lifetime on dissolved gas concentration follows $t_l \sim c_o^{-3/2}$, which fits well with the experimental results. Our findings may provide new insight on bubble and foam stability. Especially, carbonated beverages are often oversaturated, thus the extend of oversaturation may influence the stability of the foam.

5. Data Availability

The data supporting this study's findings are available from the corresponding author upon reasonable request.

6. Author Contributions

Xin Li: Investigation, Data curation, Visualization, Writing original draft. **Yanshen Li:** Conceptualization, Methodology, Supervision, Writing – review and editing.

7. Acknowledgments

We acknowledge the financial support from the National Natural Science Foundation of China under grant No. 12272376.

References

- Adami, N., Caps, H., 2015. Surface tension profiles in vertical soap films. *Phys. Rev. E* 91, 013007.
- Ardo, S., Rivas, D.F., Modestino, M.A., Greiving, V.S., Abdi, F.F., Llado, E.A., Artero, V., Ayers, K., Battaglia, C., Becker, J.P., et al., 2018. Pathways to electrochemical solar-hydrogen technologies. *Energy Environ. Sci.* 11, 2768–2783.
- Botta, O.D., MAGOS, I., Balan, C., 2020. Experimental study on the formation and break-up of fluid bubbles. *INCAS BULLETIN* 12, 27–34.
- Chatenet, M., Pollet, B.G., Dekel, D.R., Dionigi, F., De-seure, J., Millet, P., Braatz, R.D., Bazant, M.Z., Eik-erling, M., Staffell, I., et al., 2022. Water electrolysis: from textbook knowledge to the latest scientific strategies and industrial developments. *Chem. Soc. Rev.* 51, 4583–4762.
- Debrégeas, G.d., De Gennes, P.G., Brochard-Wyart, F., 1998. The life and death of "bare" viscous bubbles. *Science* 279, 1704–1707.
- Deike, L., 2022. Mass transfer at the ocean–atmosphere interface: the role of wave breaking, droplets, and bubbles. *Annu. Rev. Fluid Mech.* 54, 191–224.
- Dollet, B., Marmottant, P., Garbin, V., 2019. Bubble dynamics in soft and biological matter. *Annu. Rev. Fluid Mech.* 51, 331–355.
- Epstein, P.S., Plesset, M.S., 1950. On the stability of gas bubbles in liquid-gas solutions. *Journal of Chemical physics* 18, 1505–1509.
- Fang, Z., Wang, L., Wang, X., Zhou, L., Wang, S., Zou, Z., Tai, R., Zhang, L., Hu, J., 2018. Formation and Stability of Surface/Bulk Nanobubbles Produced by Decompression at Lower Gas Concentration. *J. Phys. Chem. C* 122, 22418–22423.
- Garbin, V., Bothe, D., Brenn, G., Casciola, C.M., Colin, C., Marengo, M., Risso, F., Tryggvason, G., Lohse, D., 2025. Bubbles and bubbly flows. *Int. J. Multiph. Flow* 190.
- Haynes, W.M., 2016. *CRC handbook of chemistry and physics*. CRC press.
- Jin, N., Zhang, F., Cui, Y., Sun, L., Gao, H., Pu, Z., Yang, W., 2022. Environment-friendly surface cleaning using micro-nano bubbles. *Particuology* 66, 1–9.
- Lhuissier, H., Villermaux, E., 2012. Bursting bubble aerosols. *J. Fluid Mech.* 696, 5–44.
- Lohse, D., 2018. Bubble puzzles: From fundamentals to applications. *Physical Review Fluids* 3.
- Lohse, D., 2022. Fundamental fluid dynamics challenges in inkjet printing. *Annu. Rev. Fluid Mech.* 54, 349–382.
- Lohse, D., Villermaux, E., 2020. Double threshold behavior for breakup of liquid sheets. *Proc. Natl. Acad. Sci. U. S. A.* 117, 18912–18914.
- Lorenceanu, E., Rouyer, F., 2020. Lifetime of a single bubble on the surface of a water and ethanol bath. *Phys. Rev. Fluids* 5, 063603.
- Magdalena, A., Pablo, H., 2017. Effects of salinity on surface lifetime of large individual bubbles. *Journal of Marine Science and Engineering* 5, 41–.
- Menesses, M., Roché, M., Royon, L., Bird, J.C., 2019. Surfactant-free persistence of surface bubbles in a volatile liquid. *Phys. Rev. Fluids* 4, 100506.
- Mohanty, R.L., Das, M.K., 2017. A critical review on bubble dynamics parameters influencing boiling heat transfer. *Renewable and Sustainable Energy Reviews* 78, 466–494.
- Nath, S., Ricard, G., Jin, P., Bouillant, A., Quéré, D., 2022. Thermal marangoni bubbles. *Soft Matter* 18, 7422–7426.
- Oratis, A.T., Bush, J.W., Stone, H.A., Bird, J.C., 2020. A new wrinkle on liquid sheets: Turning the mechanism of viscous bubble collapse upside down. *Science* 369, 685–688.

- Peleka, E.N., Gallios, G.P., Matis, K.A., 2018. A perspective on flotation: A review. *J. Chem. Technol. Biotechnol.* 93, 615–623.
- Poulain, S., Villiermaux, E., Bourouiba, L., 2018. Ageing and burst of surface bubbles. *J. Fluid Mech.* 851, 636 – 671.
- Sonin, A., Bonfillon, A., Langevin, D., 1993. Role of surface elasticity in the drainage of soap films. *Phys. Rev. Lett.* 71, 2342.
- Taylor, G.I., 1956. Fluid flow in regions bounded by porous surfaces. *Proceedings of the Royal Society of London. Series A. Mathematical and Physical Sciences* 234, 456–475.
- Viejo, C.G., Torrico, D.D., Dunshea, F.R., Fuentes, S., 2019. Bubbles, foam formation, stability and consumer perception of carbonated drinks: A review of current, new and emerging technologies for rapid assessment and control. *Foods* 8.
- Yang, G., Zhang, W., Binama, M., Li, Q., Cai, W., 2023. Review on bubble dynamic of subcooled flow boiling-part b: Behavior and models. *International Journal of Thermal Sciences* .